tion bubble; the computed sonic line did not extend as far upstream as the measured sonic line. The discrepancy is probably caused by the presence of a larger separation bubble in the experimental field, as is consistent with the higher experimental freestream flow deflection angle of 11°.

Numerical and experimental surface-pressure distributions are shown in Fig. 3 (the experimental flow deflection angle was 10°). It can be seen that AFTON-computed surface pressures fall within the scatter of experimental data and display several significant features of the observed flow, namely: 1) Inflection points of the pressure distribution are found downstream of the steep initial pressure rise. 2) The computed separation point occurs where the ratio of surface to freestream pressure, p_w/p_0, is 2.07, a value within 8% of that measured. 3) The calculated value of p_w/p_0 of 2.63 at the reattachment point differs by less than 5% from the corresponding experimental ratio. 4) The computed and measured pressures approach a common limit with increasing downstream distance from the point of reattachment; the corresponding inviscid limit is higher than in the viscous case at hand.

As in all past Saffman-model applications, no adjustment of the universal constants appearing in the model has been made to force agreement with experimental data. Results obtained indicate that, with no adjustable parameters, the Saffman turbulence model provides an accurate description of flow structure for shock-induced turbulent boundary-layer separation.

References

[1] Trulio, J. G. and Walitt, L., "Numerical Calculations of Viscous Compressible Fluid Flow Around a Stationary Cylinder," CR-1465, 1970, NASA.

[2] Trulio, J. G., Walitt, L., and Niles, W. J., "Numerical Calculations of Viscous Compressible Fluid Flow Over a Flat Plate and Step Geometry," CR-1466, 1970, NASA.

[3] Saffman, P. G., "A Model for Inhomogeneous Turbulent Flow," *Proceedings of the Royal Society*, London, Vol. A317, 1970, pp. 417–433.

[4] Wilcox, D. C. and Alber, I. E., "A Turbulence Model for High Speed Flows," *Proceedings of the 1972 Heat Transfer and Fluid Mechanics Institute*, 1972, pp. 231–252.

[5] Schlichting, H., *Boundary Layer Theory*, 4th ed., McGraw-Hill, New York, 1960, p. 367.

[6] Reda, D. C. and Murphy, J. D., "Shock Wave/Turbulent Boundary-Layer Interactions in Rectangular Channels," *AIAA Journal*, Vol. 11, No. 2, Feb. 1973, pp. 139–140.

[7] Bogdonoff, S. M. and Kepler, C. E., "Separation of a Supersonic Turbulent Boundary Layer," *Journal of Aeronautical Science*, Vol. 22, 1955, pp. 414–424.

Reynolds Stress Measurements in a Hypersonic Boundary Layer

A. DEMETRIADES* AND A. J. LADERMAN†

Philco-Ford Corporation, Newport Beach, Calif.

Introduction

THE steady-state momentum equation for the turbulent boundary layer contains contributions from the flow fluctuations which can be expressed as

$$(\partial/\partial y)(\bar{\rho}\cdot\overline{u'v'}+\bar{u}\cdot\overline{\rho'v'})$$

where the mean velocity $\bar{u}$ and the fluctuation u' are aligned with the surface, ρ' is the fluctuation around the mean density $\bar{\rho}$, and v' is the transverse velocity fluctuation aligned with the direction y normal to the surface.

Since ρ' is of the order of $(\gamma-1)M^2u'$, at low speeds, where the local Mach number approaches zero, the term $\overline{\rho'v'}$ is justifiably neglected in favor of the "Reynolds stress" $\overline{u'v'}$. By the same token, however, the importance of these two terms is reversed in hypersonic boundary layers. A long-needed demonstration of the usefulness of the hot-wire anemometer in providing quantitative turbulence data in hypersonic, compressible boundary layers has been provided recently in Ref. 1. Based on the skills developed in that investigation, the classical X-array hot-wire probe technique has been extended to the measurement of the components $\overline{u'v'}$ and $\overline{\rho'v'}$ of the Reynolds stress. The present Note describes the results obtained from this study.

Theory of X-Probe Response in Compressible Flow

The theory of the X-probe response in compressible flow, including allowances for pressure fluctuations p', has been described in detail in Ref. 2. The resulting equations and their subsequent manipulations to extract the shear stress terms are very complex, and are briefly summarized below for the simplest limit of $p'=0$. In this case, the instantaneous response of hot-wires 1 and 2 of the X-probe is given by

$$e_i(t)=e_{\tau i}[u(t)+v(t)\cot\phi_i]+e_{\sigma i}\theta(t);\quad i=1\text{ and }2 \tag{1}$$

where ϕ_i is the angle formed by the wire and the mean flow velocity vector, $e_i(t)$ is the normalized voltage fluctuation, $e_{\tau i}$ is the usual hot-wire sensitivity to velocity fluctuations in compressible flow, and $e_{\sigma i}$ is the corresponding sensitivity to static temperature fluctuations. $u(t)$ stands for $u'(t)/\bar{u}$, the local instantaneous velocity fluctuation divided by the mean, and $v(t)$ and $\theta(t)$ are defined in a similar manner. As usual, a third relation is supplied by the correlation $e_1(t)e_2(t)$ of the hot-wire signals. After some algebra these expressions can be put in the familiar form[3,4] involving the modal variables X and Y:

$$Y_1^2\equiv[\overline{e_1/e_{\sigma 1}}]^2=A_1X_1^2+A_2X_1+A_3 \tag{2}$$

$$Y_2^2\equiv[\overline{e_2/e_{\sigma 2}}]^2=B_1X_2^2+B_2X_2+B_3 \tag{3}$$

$$Z\equiv\overline{e_1e_2}/e_{\sigma_1}e_{\sigma_2}=X_1(X_2C_1+C_2)+X_2D_2+D_3 \tag{4}$$

where

$$X_1\equiv e_{\tau_1}/e_{\sigma_1},\qquad X_2\equiv e_{\tau_2}/e_{\sigma_2}$$

and

$$A_1=\overline{u^2}+\cot^2\phi_1\,\overline{v^2}+2\cot\phi_1\,\overline{uv} \tag{5a}$$

$$B_1=\overline{u^2}+\cot^2\phi_2\,\overline{v^2}+2\cot\phi_2\,\overline{uv} \tag{5b}$$

$$C_1=\overline{u^2}+\cot\phi_1\cot\phi_2\,\overline{v^2}+(\cot\phi_1+\cot\phi_2)\,\overline{uv} \tag{5c}$$

$$A_2=C_2=\overline{u\theta}+\cot\phi_1\,\overline{v\theta} \tag{6a}$$

$$B_2=D_2=\overline{u\theta}+\cot\phi_2\,\overline{v\theta} \tag{6b}$$

$$A_3=B_3=D_3=\overline{\theta^2} \tag{7}$$

Equations (2) and (3) can be solved for the A_i's and B_i's by operating each hot-wire at a minimum of three overheat currents as usual. Similarly, Eq. (4) can be solved for C_i and D_i by using the method of Ref. 4. To improve the accuracy of these operations in the present experiment, the first wire ($\phi_1\simeq 45°$) was operated at a total of 15 overheat currents, i_1, while wire no. 2 ($\phi_2\simeq 135°$) was operated at 5 currents, each of which was held constant while i_1 was varied three times; the coefficients of the resulting overdetermined set of equations were determined by the method of least squares.

The Experiment

The experiment was performed in the turbulent boundary layer

Received June 4, 1973. This work was supported by the U.S. Air Force Space and Missile Systems Organization under Contract F04701-71-C-0035.

Index categories: Boundary Layers and Convective Heat Transfer—Turbulent; Jets, Wakes, and Viscid-Inviscid Flow Interactions.

* Supervisor, Fluid Mechanics Section. Associate Fellow AIAA.

† Principal Scientist, Fluid Mechanics Section. Member AIAA.

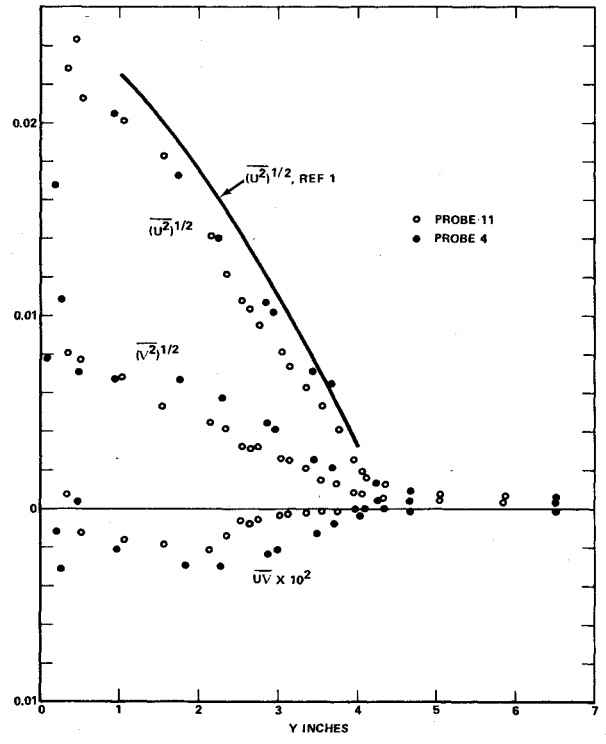

Fig. 1 Distribution of velocity fluctuations and correlation $\overline{uv}$ across the boundary layer.

growing over the ceiling of the 21-in. hypersonic wind tunnel of the Jet Propulsion Laboratory. Flow conditions for these tests were the same as those in Ref. 5, i.e., $M_\infty = 9.4$, $T_0 = 790°K$, $P_0 = 3200$ cm Hg. Under these conditions mean-flow measurements have shown that the boundary layer is 10 cm thick with a momentum Reynolds number $R_\theta = 37{,}000$. The X-array anemometer probe used for the shear stress measurements consisted of two hot-wire elements, 0.00001 in. in diameter by approximately 0.003–0.004 in. long. Details of the probe construction are similar to those described in Ref. 6. Data was acquired by locating the probe at each of about 40 y-positions above the surface and, for each combination of hot-wire currents, tape-recording the wire mean and a.c. signals for 10 sec at 60 ips. Heat-transfer calibrations of the individual hot-wires were obtained from freestream measurements made immediately prior to the test and from current-resistence characteristics determined from the boundary-layer overheat traverses.

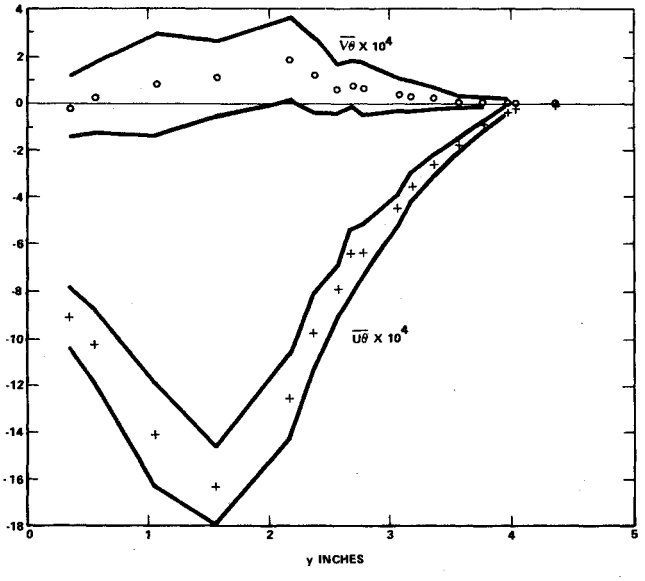

Fig. 2 Velocity temperature correlations. Symbols denote the average of four calculations [see Eqs. (6)] while solid lines represent the maximum and minimum values.

Results

The earlier experiments of Ref. 1 with the same boundary-layer disclosed that the pressure fluctuations p' were dominant throughout the layer. On the other hand, the velocity and temperature fluctuations did not appear sensitive to the inclusion ($p' \neq 0$) or exclusion ($p' = 0$) of the pressure fluctuations in the data-reduction process. Thus, while the complete solution allowing for p' was yet to come, it was felt that the analysis of the preceding paragraphs assuming $p' = 0$ would give also a reasonable estimate of the shear terms. This approach was also justified a posteriori since, as we shall see below, the resulting u' and θ' data agree with the corresponding data from Ref. 1.

Using this approach, the coefficients on the left-hand side of Eqs. (5–7) were computed as a function of y and at each position the equations were solved for the six turbulence terms. At this point, it should be emphasized that errors inherent in the measurements and introduced by the several least squares procedures will reflect in the various coefficients. It can be expected therefore that A_2 (or B_2) will not identically equal C_2 (or D_2). As shown below $\overline{v\theta}$ is smaller than $\overline{u\theta}$ and since it is proportional to the difference between two relatively large numbers (e.g., $\overline{v\theta} \propto A_2 - B_2$), small errors in the coefficients can appear as large uncertainties in $\overline{v\theta}$. In addition, $\overline{uv} < \overline{v^2} < \overline{u^2}$ and as a result $\overline{uv}$ exhibits the largest sensitivity to small uncertainties in the coefficients A_1, B_1 and C_1. Consequently, considerable caution and judgement must be exercised in assessing the validity of the data and in interpreting the results of the analysis.

The rms temperature fluctuations determined from the coefficients A_3, B_3 and D_3 were each found to be in reasonable

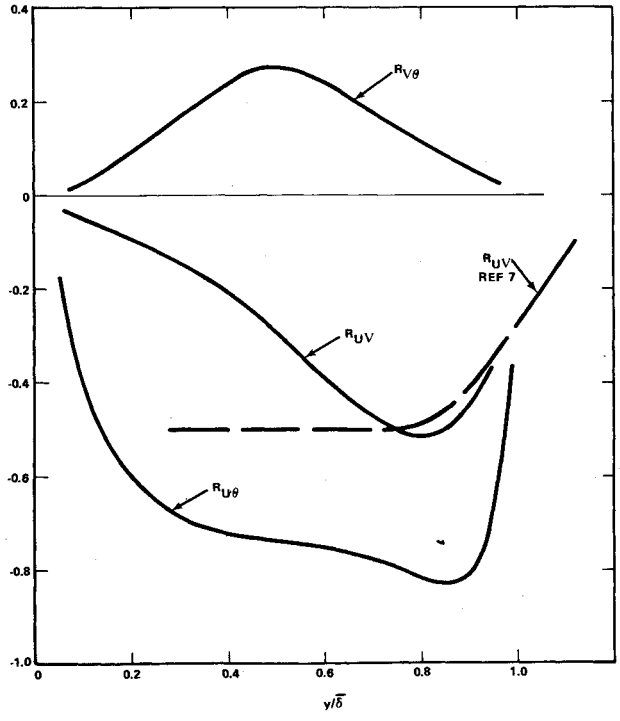

Fig. 3 Distribution of the correlation coefficients across the boundary layer.

agreement with each other and with those of Ref. 1. Results for the rms velocity fluctuations and $\overline{uv}$, taken with two different X-probes (marked no. 4 and no. 11), are plotted on Fig. 1 which shows that, except for the correlation, the results obtained from the two probes are in remarkably good agreement. The discrepancy in $\overline{uv}$ [which is the smallest of the three terms determined from Eqs. (5)] is more a consequence of uncertainties in the data rather than differences in the probe response. The cross-correlations $\overline{u\theta}$ and $\overline{v\theta}$ are shown in Fig. 2 where the average value and range of the four possible solutions are presented. Since $\overline{u\theta}$ is of the same sign and similar magnitude as the governing coefficients, the uncertainties in the former are similar to those in the latter. The $\overline{v\theta}$ term, on the other hand, is considerably smaller and even small errors in the coefficients are translated as large uncertainties in this quantity. It appears, however, that $\overline{v\theta}$ is positive through the boundary layer and approximately 10 times larger than $\overline{uv}$. Finally, Fig. 3 shows the correlation coefficients, defined by $R_{uv} = \overline{uv}/[(u^2)(v^2)]^{1/2}$, and similarly for $R_{u\theta}$ and $R_{v\theta}$ resulting from Fig. 2.

In comparison with other data, it is of interest to note that at low speeds[7,8] $(\overline{v^2})^{1/2}$ is approximately 60–70% of $(\overline{u^2})^{1/2}$, while the correlation coefficient $R_{uv} \simeq -0.5$ throughout the boundary layer (see Fig. 3). In the present case, $(\overline{v^2})^{1/2}$ varies from $\frac{1}{4}$ to $\frac{1}{3}$ of $(\overline{u^2})^{1/2}$, indicating that the departure from isotropy becomes appreciably larger at hypersonic speeds. Furthermore, while R_{uv} reaches a peak of -0.5 near the outer edge of the boundary layer, in contrast to the low-speed case, it then decreases steadily to zero as the wall is approached. While it is somewhat premature to draw general conclusions from the aforementioned comparison, the present results have indicated significant differences from the low-speed boundary layer, which should find application in the refinement of analytical techniques for modeling hypersonic shear flows.

References

[1] Laderman, A. J. and Demetriades, A., "Hot-Wire Measurements of Hypersonic Boundary-Layer Turbulence," *The Physics of Fluids*, Vol. 16, No. 2, Feb. 1973, pp. 179–181.

[2] Demetriades, A. and Laderman, A. J., "Final Progress Report; Advanced Penetration Problems Project," SAMSO Rept. 73-129, Feb. 1973, Philco-Ford Corp., Newport Beach, Calif.

[3] Morkovin, M. V., "Fluctuations and Hot-Wire Anemometry in Compressible Flows," AGARDograph 24, 1956.

[4] Demetriades, A., "Theory of Hot-Wire Correlation Measurements in Compressible Flow with Application to Wakes," AIAA Paper 72-177, San Diego, Calif., 1972.

[5] Laderman, A. J. and Demetriades, A., "Mean Flow Measurements in a Hypersonic Turbulent Boundary-Layer," Publ. U-4950, Aug. 1971, Philco-Ford Corp., Newport Beach, Calif.

[6] Doughman, E. L., "Development of a Hot-Wire Anemometer for Hypersonic Turbulent Flows," *Review of Scientific Instruments*, Vol. 43, No. 8, Aug. 1972, pp. 1200–1202.

[7] Klebanoff, P. S., "Characteristics of Turbulence in a Boundary-Layer with Zero Pressure Gradient," TR 1247, 1955, NACA.

[8] Sandborn, V. A. and Braun, W. H., "Turbulent Shear Spectra and Local Isotropy in the Low Speed Boundary-Layer," TN-3761, 1956, NACA.